

## Research Article

# Fourier Transform Infrared Spectroscopy of “Bisphenol A”

Ramzan Ullah,<sup>1,2</sup> Ishaq Ahmad,<sup>2</sup> and Yuxiang Zheng<sup>1</sup>

<sup>1</sup>Shanghai Ultra-Precision Optical Manufacturing Engineering Center, Department of Optical Science and Engineering, Fudan University, Shanghai 200433, China

<sup>2</sup>Department of Physics, COMSATS Institute of Information Technology, Islamabad 45550, Pakistan

Correspondence should be addressed to Ramzan Ullah; ramzanullah@gmail.com and Yuxiang Zheng; yxzhang@fudan.edu.cn

Received 2 May 2016; Revised 2 July 2016; Accepted 19 July 2016

Academic Editor: Eugen Culea

Copyright © 2016 Ramzan Ullah et al. This is an open access article distributed under the Creative Commons Attribution License, which permits unrestricted use, distribution, and reproduction in any medium, provided the original work is properly cited.

FTIR (400–4000  $\text{cm}^{-1}$ ) spectra of “Bisphenol A” are presented. Absorption peaks (400–4000  $\text{cm}^{-1}$ ) are assigned on the basis of Density Functional Theory (DFT) with configuration as B3LYP 6-311G++ (3df 3pd). Calculated absorption peaks are in reasonable reconciliation with experimental absorption peaks after scaling with scale factor of 0.9679 except C-H and O-H stretching vibrations.

## 1. Introduction

“Bisphenol A” is a carbon based synthetic compound used primarily in the plastic industry and epoxy resins. BPA mimics hormone-like behavior which questions upon its use in food containers and baby bottles and so forth. BPA has been controversially associated with a number of adverse health effects including neurotoxicity, genotoxicity, and carcinogenicity [1]. BPA ( $\text{C}_{15}\text{H}_{16}\text{O}_2$ ) molecule is shown in Figure 1. BPA has been used tremendously in many areas like optical media, food containers, medical devices, electronics, protective coatings, and automotive industry are very few to mention. Besides that, the debate over the use of BPA for public health safety continues where US Food and Drug Administration (FDA) considers BPA totally safe for food containers and packaging [2] but some other researches oppose this idea [3]. In this state of perplexity, banning the use of BPA in some applications mostly related to foods and human contact is on the rise [4]. Situation further gets worse when some researches show that “Bisphenol S” is also toxic like BPA which is a common replacement for BPA to bypass the law [5]. Keeping in view its widespread use and significance, its optical properties are very important. Some environmental hormones have already been studied by THz, Raman, and FTIR spectroscopy [6]. BPA has also been studied by THz spectroscopy where one of its vibrational modes was observed but in FTIR spectroscopy, main focus was on

CH and OH stretching [7]. Various molecular vibrations of BPA have been identified through Raman spectroscopy by our research group [8]. However, Raman spectroscopy and FTIR spectroscopy are complementary to each other. To get a complete picture of the molecular dynamics, both Raman and FTIR spectroscopic studies are essential. So, here we present a complementary FTIR spectroscopic study of BPA which will help a lot to understand the behavior of this molecule to a wide extent. The goal of this study is to find molecular vibrations of BPA in the Infrared regime which will pave the way to a better understanding of the interaction of this molecule and in finding the origin of its toxicity. This study may also help researchers and health agencies to devise better ways for the characterization and detection of BPA.

## 2. Experimental Set-Up

Spectrum 100 FTIR [9] from PerkinElmer is used to record the spectra from 400 to 4000  $\text{cm}^{-1}$ . BPA, CAS number (80-5-7), is purchased from “Sinopharm Chemical Reagent Co. Ltd.” [10]. Sample as well as Potassium Bromide (KBr) is ground to very fine powder and then a tablet is formed under high pressure after mixing them. This tablet is then put on the optical path of Infrared radiation to take the measurements. All the measurements were taken at room temperature and atmospheric pressure.

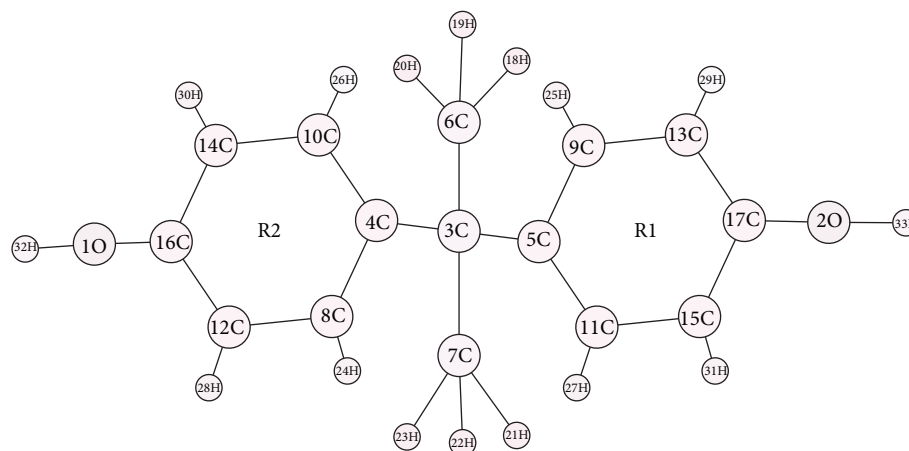


FIGURE 1: Bisphenol A molecule.

### 3. DFT Calculations

Gaussian 09 package [11] is utilized to carry out DFT related calculations which are optimized to minimum and Ground State method B3LYP with 6-311G basis set [12] is used together with (3df, 3pd) and ++ diffuse functions [13]. MOLVIB [14, 15] is used to calculate Potential Energy Distributions (PEDs) given in Table 1. Another table given in the Supplementary Material contains more information about simulation and values of important parameters obtained like energy, dipole moment and so forth (see Supplementary Material available online at <http://dx.doi.org/10.1155/2016/2073613>).

### 4. Results and Discussion

Figure 2 shows experimental spectra of “Bisphenol A” in the range  $400\text{--}1700\text{ cm}^{-1}$  along with calculated DFT spectra in absorbance mode for easy comparison. Absorption peaks are reasonably in good agreement in the region  $400\text{ to }1700\text{ cm}^{-1}$  after scaling with scale factor of 0.9679 for vibrational frequencies calculated by Andersson and Uvdal [16]. However, the large deviation of experimental C-H and O-H stretching vibrations with the DFT peaks as shown in Figure 3 has been addressed by Ullah et al. [7].

Experimental peak of  $531\text{ cm}^{-1}$  is assigned to  $543\text{ cm}^{-1}$  B3LYP which is a combination of different motions including CO, CC out of plane bending, and CCC interactions in both the rings and otherwise.  $531\text{ cm}^{-1}$  experimental absorption peak is not clearly visible in Figure 2 which lies behind  $552\text{ cm}^{-1}$ . It is clear from Table 1 that  $552\text{ cm}^{-1}$  and  $564\text{ cm}^{-1}$  experimental peaks are mainly due to CO, CC, and CH out of plane bending along with little amount of torsions in both the rings and hence are assigned to  $563\text{ cm}^{-1}$  and  $572\text{ cm}^{-1}$  (B3LYP), respectively, as shown in Figure 2. FTIR absorption peak of  $721\text{ cm}^{-1}$ , which, according to Table 1, is assigned to simulated value of  $734\text{ cm}^{-1}$  and corresponding PED analysis shows that the major contribution in this vibrational mode comes from the torsions in both the rings and CC out of plane bending. Absorption peak of  $734\text{ cm}^{-1}$  is assigned to  $768\text{ cm}^{-1}$  which is caused by CC stretching. Next absorption

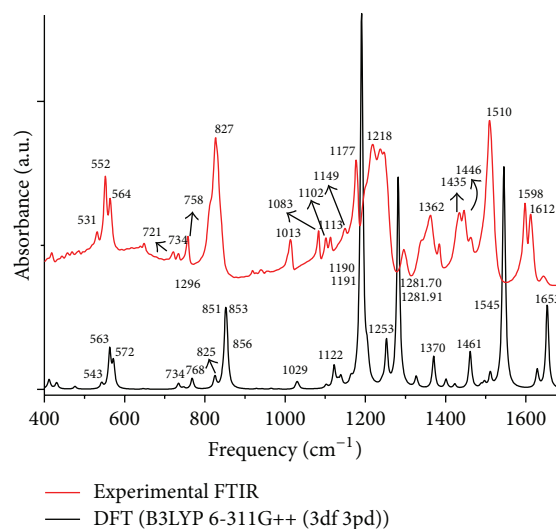


FIGURE 2: FTIR ( $400\text{--}1700\text{ cm}^{-1}$ ) spectra of “Bisphenol A” along with DFT spectra. Values of some peaks are given near the tip of the respective peak.

peak,  $758\text{ cm}^{-1}$  which is clearly marked with its value in Figure 2, is really interesting to see that it is due to the CH out of plane bending motion and we can clearly see that there is only one experimental peak with this value but B3LYP shows two distinct peaks of  $825\text{ cm}^{-1}$  and  $826\text{ cm}^{-1}$  in Table 1. Hence, we assign  $758\text{ cm}^{-1}$  to both of these values. Moreover, this CH out of plane bending does not come from single carbon and hydrogen atoms. It is actually the combination of all the CH out of plane bending motions in both the rings. A relatively high absorption peak of  $827\text{ cm}^{-1}$  (Figure 2) is assigned to 4 simulated vibrational modes of  $844$ ,  $851$ ,  $853$ , and  $856\text{ cm}^{-1}$  due to their closeness. The major contribution in  $844\text{ cm}^{-1}$  mode is from CO stretching and CC stretching in both the rings. The other three come mainly from CH out of plane bending movements. So the experimental peak  $827\text{ cm}^{-1}$  might belong to any of them. In a similar fashion,  $1013\text{ cm}^{-1}$  is assigned to 3 simulated values of  $1026$ ,  $1029$ , and  $1033\text{ cm}^{-1}$ . Interestingly, the first and

TABLE I: Experimental as well as DFT absorption peaks along with PEDs.

Sr. number	Experimental FTIR (cm <sup>-1</sup> )	Simulated (B3LYP) cm <sup>-1</sup>	PED (%)
1	531	543	$\nu$ CCC4 (36), $\gamma$ COob (12), $\nu$ CCCR2 (9), $\nu$ CCCR1 (9), $\gamma$ CCob (5)
2	552	563	$\gamma$ COob (28), $\gamma$ CCob (15), $\nu$ CCC4 (14), $\gamma$ CHob (12), $\tau$ R1t (7), $\tau$ R2t (6)
3	564	572	$\gamma$ COob (34), $\gamma$ CHob (15), $\gamma$ CCob (13), $\nu$ CCC4 (12), $\tau$ R2t (9), $\tau$ R1t (8)
4	721	734	$\tau$ R1t (23), $\tau$ R2t (23), $\gamma$ COob (20), $\gamma$ CCob (19), $\gamma$ CHob (7)
5	734	768	$\nu$ CC4 (26), $\nu$ CCC4 (20), $\nu$ CO (8), $\delta$ CCHb (6), $\nu$ CCHa (6), $\nu$ CCCR1 (5)
6	758	825	$\gamma$ CHob (95)
7	758*	826	$\gamma$ CHob (95)
8	827	844	$\nu$ CO (23), $\nu$ CCR2 (14), $\nu$ CCR1 (14), $\nu$ CCCR2 (12), $\nu$ CCCR1 (12), $\nu$ CC4 (6)
9	827*	851	$\gamma$ CHob (43), $\nu$ CO (9), $\nu$ CCR2 (9), $\nu$ CCR1 (8), $\gamma$ COob (6)
10	827*	853	$\gamma$ CHob (70), $\gamma$ COob (11)
11	827*	856	$\gamma$ CHob (52), $\gamma$ COob (8), $\nu$ CCR1 (5), $\nu$ CO (5), $\nu$ CCR2 (5)
12	1013	1026	$\nu$ CCHa (28), $\nu$ CCHb (28), $\nu$ CCCR1 (8), $\nu$ CCCR2 (7), $\nu$ CCR1 (7), $\nu$ CCR2 (6)
13	1013*	1029	$\nu$ CCCR1 (21), $\nu$ CCCR2 (21), $\nu$ CCR1 (15), $\nu$ CCR2 (15), $\nu$ CCHR1 (12), $\nu$ CCHR2 (11)
14	1013*	1033	$\nu$ CCHa (16), $\nu$ CCHb (16), $\nu$ CCCR2 (13), $\nu$ CCCR1 (11), $\nu$ CCR2 (11), $\nu$ CCR1 (9)
15	1083	1122	$\nu$ CC4 (26), $\nu$ CCR1 (12), $\nu$ CCR2 (12), $\nu$ CCHR1 (9), $\nu$ CCHR2 (9), $\nu$ CCC4 (7)
16	1102	1132	$\nu$ CCR2 (15), $\nu$ CCR1 (15), $\nu$ CCHR2 (15), $\nu$ CCHR1 (15), $\nu$ CC4 (10), $\nu$ CCHb (7)
17	1113	1139	$\nu$ CCHR2 (16), $\nu$ CCHR1 (16), $\nu$ CCR2 (14), $\nu$ CCR1 (14), $\nu$ CCHa (9), $\nu$ CCHb (9)
18	1149	1164	$\nu$ CC4 (29), $\nu$ CCC4 (17), $\nu$ CCHR2 (12), $\nu$ CCHR1 (12), $\nu$ CCR2 (7), $\nu$ CCR1 (7)
19	1177	1190	$\nu$ COH (55), $\nu$ CCR1 (12), $\nu$ CCR2 (8), $\nu$ CO (7), $\nu$ CCHR1 (7)
20	1177*	1191	$\nu$ COH (56), $\nu$ CCR2 (13), $\nu$ CCR1 (10), $\nu$ CCHR2 (7), $\nu$ CO (6), $\nu$ CCHR1 (5)
21	1218	1253 (Tentative)	$\nu$ CC4 (45), $\nu$ CCC4 (13), $\nu$ CCHa (8), $\nu$ CCHb (8), $\nu$ CCR1 (6), $\nu$ CCR2 (6)
22	1218*	1281.70 (Tentative)	$\nu$ CO (55), $\nu$ CCR2 (10), $\nu$ CCR1 (9), $\nu$ CCHR2 (8), $\nu$ CCHR1 (7)
23	1218*	1281.91 (Tentative)	$\nu$ CO (54), $\nu$ CCR1 (9), $\nu$ CCHR1 (9), $\nu$ CCR2 (8), $\nu$ CCHR2 (8)
24	1296	1326	$\nu$ CCR1 (31), $\nu$ CCR2 (29), $\nu$ CCC4 (12), $\nu$ CCHR1 (9), $\nu$ CCHR2 (8)
25	1362	1370.15	$\nu$ CCHR2 (32), $\nu$ CCHR1 (20), $\nu$ COH (16), $\nu$ CCR2 (16), $\nu$ CCR1 (9)
26	1362*	1370.41	$\nu$ CCHR1 (33), $\nu$ CCHR2 (20), $\nu$ COH (17), $\nu$ CCR1 (16), $\nu$ CCR2 (10)
27	1384	1401	$\delta$ HCHb (23), $\delta$ CCHb (23), $\nu$ HCHa (22), $\nu$ CCHa (22), $\nu$ CC4 (5)
28	1435	1461	$\nu$ CCR2 (26), $\nu$ CCHR2 (24), $\nu$ CCR1 (11), $\nu$ CCHR1 (11), $\nu$ CCC4 (10), $\nu$ COH (9)
29	1446	1462	$\nu$ CCR1 (26), $\nu$ CCHR1 (25), $\nu$ CCR2 (11), $\nu$ CCHR2 (11), $\nu$ COH (9), $\nu$ CCC4 (8)
30	1463	1510.8	$\nu$ HCHa (44), $\nu$ HCHb (44)
31	1463*	1511.55	$\nu$ HCHb (46), $\nu$ HCHa (45)
32	1510	1545	$\nu$ CCHR2 (26), $\nu$ CCHR1 (24), $\nu$ CCR2 (16), $\nu$ CCR1 (14), $\nu$ CO (8)
33	1510*	1548	$\nu$ CCHR1 (26), $\nu$ CCHR2 (24), $\nu$ CCR1 (16), $\nu$ CCR2 (15), $\nu$ CO (8)
34	1598	1628	$\nu$ CCR1 (33), $\nu$ CCR2 (33), $\nu$ CCHR1 (7), $\nu$ CCHR2 (7), $\nu$ COH (6)
35	1612	1653	$\nu$ CCR2 (39), $\nu$ CCR1 (22), $\nu$ CCHR2 (14), $\nu$ CCHR1 (8), $\nu$ CCCR2 (6)
36	1612*	1654	$\nu$ CCR1 (39), $\nu$ CCR2 (22), $\nu$ CCHR1 (14), $\nu$ CCHR2 (8), $\nu$ CCCR1 (6)
37	2870	3029	$\nu$ CH3a (59), $\nu$ CH3b (41)
38	2870*	3034	$\nu$ CH3b (59), $\nu$ CH3a (41)
39	2933	3093	$\nu$ CH3a (57), $\nu$ CH3b (42)
40	2964	3098	$\nu$ CH3b (56), $\nu$ CH3a (44)
41	2975	3104	$\nu$ CH3a (77), $\nu$ CH3b (22)
42	2975*	3105	$\nu$ CH3b (79), $\nu$ CH3a (20)
43	3337	3833.87	$\nu$ OH (100)
44	3337*	3834.41	$\nu$ OH (100)

\* Multiple assignments.

Ob: out of plane bending; t and  $\tau$ : torsion. R1: Ring 1, R2: Ring 2, a: Label a, b: Label b,  $\nu$ : stretching,  $\delta$ : in-plane deformation,  $\gamma$ : out-of-plane deformation, and R: ring.

Scale factor for DFT B3LYP 6-311++G (3df, 3pd) is 0.9679.

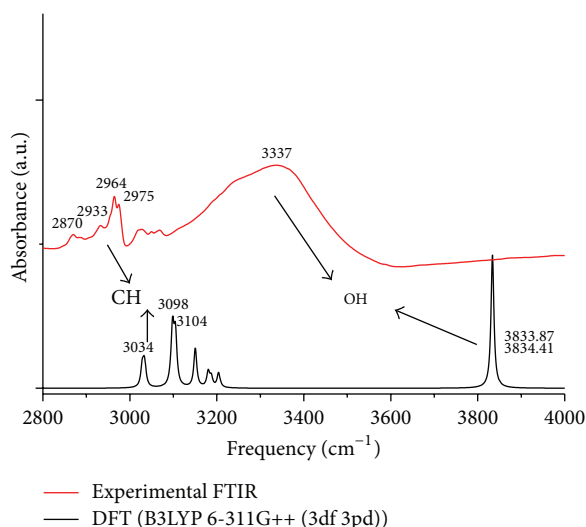


FIGURE 3: FTIR (2800–4000  $\text{cm}^{-1}$ ) spectra of “Bisphenol A” along with DFT spectra. Values of some peaks are given near the tip of the respective peak.

last peaks (1026 and 1033  $\text{cm}^{-1}$ ) have similar contributions as given by PED analysis in Table 1 but the middle one 1029  $\text{cm}^{-1}$  has different motions. However, they are too close to each other that DFT also suggests a single experimental peak in such circumstance. So 1013  $\text{cm}^{-1}$  has once again multiple assignments. 1083  $\text{cm}^{-1}$  and 1102  $\text{cm}^{-1}$  are related to B3LYP values of 1122  $\text{cm}^{-1}$  and 1132  $\text{cm}^{-1}$ , respectively, which are contributed mostly by CC stretching in both the rings. 1113  $\text{cm}^{-1}$  and 1149  $\text{cm}^{-1}$  are hereby assigned to 1139  $\text{cm}^{-1}$  and 1164  $\text{cm}^{-1}$ , respectively, according to Table 1 and relative PED analysis shows that these modes are mainly because of CCH and CC interactions in the molecule. Multiple assignment of the experimental peak of 1177  $\text{cm}^{-1}$  to both 1190  $\text{cm}^{-1}$  and 1191  $\text{cm}^{-1}$  is due to their nearness. The respective PED analysis shows that the interactions are similar in such a way that for one DFT peak 1190  $\text{cm}^{-1}$ , it is the motion in one ring and for the other 1191  $\text{cm}^{-1}$ , it is the same motion but in the second ring. Since their frequencies are bit different, DFT gives two peaks but experimentally, it shows only one as shown in Figure 2. Immediately next to the 1177  $\text{cm}^{-1}$  peak, there is rather a broadband peak with small fluctuations in Figure 2. Its value is given in Table 1 as 1218  $\text{cm}^{-1}$  which is the highest point along the broad peak. If we compare it with DFT spectra, a small peak of 1253  $\text{cm}^{-1}$  might be assigned to it. However, due to broadband nature of this curve, it is hard to assign it with certain degree of confidence. Moreover, DFT spectra also show a rather high peak adjacent to 1253  $\text{cm}^{-1}$ , as given in Figure 2, which is actually two peaks (1281.70  $\text{cm}^{-1}$  and 1281.91  $\text{cm}^{-1}$ ) according to Table 1. These two peaks can also be assigned to 1218  $\text{cm}^{-1}$ . However, the shape of the experimental curve does not show a good behavior which might be due to some defect and hence tentative assignment is given here. PED analysis shows the former as a result of CC stretching and the last two from CO stretching. 1296  $\text{cm}^{-1}$  is assigned to 1326  $\text{cm}^{-1}$  which is

from CC stretching in two rings. 1362  $\text{cm}^{-1}$  is assigned to two absorption peaks of 1370.15  $\text{cm}^{-1}$  and 1370.41  $\text{cm}^{-1}$  resulting from CCH interactions in the rings but with different configurations. In a similar fashion, 1384  $\text{cm}^{-1}$  can be assigned to 1401  $\text{cm}^{-1}$  originating from HCH and CCH interactions. 1435  $\text{cm}^{-1}$  and 1446  $\text{cm}^{-1}$  are attributed to 1461  $\text{cm}^{-1}$  and 1462  $\text{cm}^{-1}$ , respectively, resulting from CC and CCH in the rings. 1463  $\text{cm}^{-1}$  which is not very clear in Figure 2 is assigned to two DFT peaks, 1510.8  $\text{cm}^{-1}$  and 1511.55  $\text{cm}^{-1}$ , both of which are resulting from HCH interactions (not occurring in the rings) in different ways as shown in PED analysis. A sharp absorption peak of 1510  $\text{cm}^{-1}$  in Figure 2 goes to 1545  $\text{cm}^{-1}$  and 1548  $\text{cm}^{-1}$  where CCH and CC modes are prevalent. 1598  $\text{cm}^{-1}$  is assigned to calculated frequency of 1628  $\text{cm}^{-1}$  and similarly experimental peak of 1612  $\text{cm}^{-1}$  to 1653  $\text{cm}^{-1}$  and 1654  $\text{cm}^{-1}$  (multiple). Spectra end here and after a long pause, peaks start appearing again near 3000  $\text{cm}^{-1}$  where C-H and then O-H stretching interactions exist which are clearly marked in Figure 3. The detailed analysis and assignment of these modes can be found in [6]. Spectra in the range 1700 to 2800  $\text{cm}^{-1}$  are not shown due to nonexistence of any peak.

Simulated values of B3LYP given in Table 1 are raw values. These values can be corrected by using a scale factor of 0.9679 as discussed earlier in this section. DFT values are rounded off to nearest whole number. Only major peaks are labeled in Figures 2 and 3. The detail of the absorption peaks both experimental as well as calculated is given in Table 1. Assignment is done on the basis of comparison of the relative intensities of the experimental and calculated spectra.

According to DFT calculations, there are 14 C-H stretching vibrations in different combinations between 3000 and 3300  $\text{cm}^{-1}$ . Only few of them are visible in Figure 2. As “Bisphenol A” is relatively large molecule and many peaks are very near to each other, so it is hard to assign the individual peaks distinctly without multiple assignments as indicated at the end of Table 1.

## 5. Conclusion

We have presented FTIR (400–4000  $\text{cm}^{-1}$ ) spectra of “Bisphenol A.” Peaks (400–4000  $\text{cm}^{-1}$ ) have been assigned on the basis of Density Functional Theory (DFT) with configuration as B3LYP 6-311G++ (3df 3pd). Calculated absorption peaks are in reasonable agreement with experimental peaks after scaling with scale factor of 0.9679 except C-H and O-H stretching vibrations.

## Competing Interests

The authors declare that they have no competing interests.

## Acknowledgments

This work has been partially supported by the National Natural Science Foundation of China (no. 61275160). The authors would like to thank Professor S. Y. Wang for providing computer resources.

## References

- [1] [http://www.who.int/foodsafety/publications/fs\\_management/No.05\\_Bisphenol\\_A\\_Nov09\\_en.pdf](http://www.who.int/foodsafety/publications/fs_management/No.05_Bisphenol_A_Nov09_en.pdf).
- [2] <http://www.fda.gov/Food/IngredientsPackagingLabeling/Food-AdditivesIngredients/ucm355155.htm>.
- [3] A. M. Hormann, F. S. Vom Saal, S. C. Nagel et al., "Holding thermal receipt paper and eating food after using hand sanitizer results in high serum bioactive and urine total levels of bisphenol A (BPA)," *PLoS ONE*, vol. 9, no. 10, Article ID e110509, 2014.
- [4] <http://www.bisphenol-a-europe.org/factsmyths/8/24/Certain-countries-have-banned-BPA>.
- [5] R. Viñas and C. S. Watson, "Bisphenol S disrupts estradiol-induced nongenomic signaling in a rat pituitary cell line: effects on cell functions," *Environmental Health Perspectives*, vol. 121, no. 3, pp. 352–358, 2013.
- [6] R. Ullah, S. U.-D. Khan, M. Aamir, and R. Ullah, "Terahertz time domain, Raman and fourier transform infrared spectroscopy of acrylamide, and the application of density functional theory," *Journal of Spectroscopy*, vol. 2013, Article ID 148903, 17 pages, 2013.
- [7] R. Ullah, H. Li, and Y. Zhu, "Terahertz and FTIR spectroscopy of 'Bisphenol A'" *Journal of Molecular Structure*, vol. 1059, no. 1, pp. 255–259, 2014.
- [8] R. Ullah and Y. Zheng, "Raman spectroscopy of 'Bisphenol A,'" *Journal of Molecular Structure*, vol. 1108, pp. 649–653, 2016.
- [9] <http://www.research.usf.edu/rf/docs/perkin-elmer-spectrum-100-ftir-users-guide.pdf>.
- [10] <http://en.reagent.com.cn/>.
- [11] M. J. Frisch, G. W. Trucks, H. B. Schlegel et al., *Gaussian 09, Revision A.01*, Gaussian, Inc, Wallingford, Conn, USA, 2009.
- [12] V. A. Rassolov, J. A. Pople, M. Ratner, P. C. Redfern, and L. A. Curtiss, "6-31G\* basis set for third-row atoms," *Journal of Computational Chemistry*, vol. 22, no. 9, pp. 976–984, 2001.
- [13] T. Clark, J. Chandrasekhar, G. W. Spitznagel, and P. V. Schleyer, "Efficient diffuse function-augmented basis sets for anion calculations. III. The 3-21+G basis set for first-row elements, Li-F," *Journal of Computational Chemistry*, vol. 4, no. 3, pp. 294–301, 1983.
- [14] T. Sundius, "Molvib—a flexible program for force field calculations," *Journal of Molecular Structure*, vol. 218, pp. 321–326, 1990.
- [15] T. Sundius, "A new damped least-squares method for the calculation of molecular force fields," *Journal of Molecular Spectroscopy*, vol. 82, no. 1, pp. 138–151, 1980.
- [16] M. P. Andersson and P. Uvdal, "New scale factors for harmonic vibrational frequencies using the B3LYP density functional method with the triple- $\zeta$  basis Set 6-311+G(d,p)," *Journal of Physical Chemistry A*, vol. 109, no. 12, pp. 2937–2941, 2005.

